Malaysian Simulation SOCIETY
http://www.ams-mss.org
APPLICATIONS OF MODELLING AND SIMULATION
eISSN 2600-8084
VOL 1, NO. 1, 2017, 15-21

Modelling and Sway Control of a Double-Pendulum Overhead Crane System

Tan Ying Jian and Z. Mohamed*

Faculty of Electrical Engineering, Universiti Teknologi Malaysia, 81310 UTM Skudai, Johor, Malaysia.

*Corresponding author: zahar@fke.utm.my

Abstract: A crane system is very important in industries as the system is used to transport a heavy load from one place to another. A double-pendulum type overhead crane system is very difficult to control as it suffers from payload sway and double-pendulum dynamics. These affect the system performance and the safety of the operation. This paper focuses on the mathematical modelling and sway control of a double-pendulum overhead crane system. The mathematical model of a double-pendulum overhead crane system is obtained through the Euler-Lagrange methods. The dynamic model is then verified through simulations and experiments. The simulation is carried out using the Simulink block diagram in MATLAB whereas the experiment is carried out using a laboratory overhead crane. Upon obtaining an accurate dynamic model of the double-pendulum overhead crane system, controllers based on input shaping are designed to improve the system performance.

Keywords: Double-pendulum crane; Euler-Lagrange; Modelling; Simulation; Sway control.

1. INTRODUCTION

Crane systems are commonly found in industries such as construction sites, manufacturing plants, warehouses, nuclear plants and harbour plants to handle heavy loads [1-6]. The crane system helps the industry to transport heavy loads from one place to another. A tower crane, an overhead crane and a harbour crane are amongst the famous cranes used in industries. These cranes can be categorised based on their dynamic properties and coordinate system [7]. The tower crane is mainly used in a construction site, and a cylindrical coordinate system is used to describe the coordinate and the motion of the payload during operation. The load is supported by a cable and the cart moves by the trolley along the jib arm. Besides, the overhead crane system uses the Cartesian space to describe the position and the motion of the system. The motion of the crane is perpendicular to the cart or trolley. On the other hand, the harbour crane used a spherical coordinate to describe the coordinate and motion of the system. The payload is supported by the suspension. A harbour crane is normally placed on a base for easier change of workspace.

Amongst all, the overhead crane system is the most used by crane industries especially in a manufacturing plant. The system needs to operate at a very fast, precise and accurate manner as the efficiency is directly related to productivity in industries. Most of the overhead crane systems used by the industry is a double-pendulum overhead crane system as shown in Figure 1. For a double-pendulum overhead crane system, the system is equipped with a hook and a payload attach to it. The operation of the overhead crane system become challenging due to the existing of the dynamic behaviour of the double-pendulum overhead crane.

Many previous researches carried out on the overhead crane system based on the assumption that the system is a single-pendulum model which does not always hold true. In certain cases, the hook mass cannot be ignored and this resulted in a double-pendulum type system [8]. Unlike a single-pendulum which only consist payload sway, a double-pendulum needs to consider the payload sway as well as the hook sway. It was reported that a double-pendulum type overhead crane system suffered from payload oscillations [1-2,8-10,5-7,9-12] and double-pendulum dynamics [1-2,5-9,12,14-15]. The operation takes a longer time to settle down and this increase the completion time. Therefore, obtaining a fast, precise and accurate double-pendulum overhead crane system in positioning the load with minimum payload sway become challenging due to the complexity and dynamic behavior of the double-pendulum overhead crane system.

This paper presents modelling an overhead crane with double-pendulum dynamics. The dynamic model is derived using the Euler-Lagrange method and verified with a laboratory crane. Subsequently, an input shaping techniques are designed and implemented for sway control of the crane. Simulation and experimental results are presented to investigate the performance of the input shapers.

2. RESEARCH METHODOLOGY

2.1 Mathematical Modelling

Figure 2 shows the schematic diagram of a double-pendulum overhead crane system. The system is driven by a force, F by

motor drive and with a frictional force, f_x opposed the motion of the crane. The crane consists of cart, hook and a payload. The payload is attached to the hook as shown in Figure 2. m, m_1 and m_2 represents the cart mass, hook mass and payload mass of the crane respectively. L_1 and L_2 indicate the cable lengths of the hook and the payload respectively. Three outputs of the system are the cart position, x, hook angle θ_1, and payload angle θ_2. In this work, several assumptions have been made during for modelling of the double-pendulum crane.

- The hook and the payload are assumed to be a mass-point.
- The cable for the hook and payload is assumed to be massless and inflexible.
- The elongation of the cables during the motion of the cable is neglected.

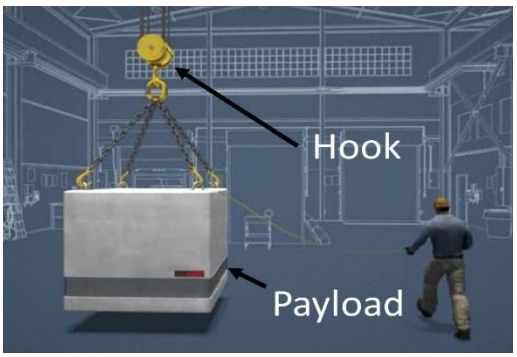

Figure 1. A double-pendulum overhead crane system

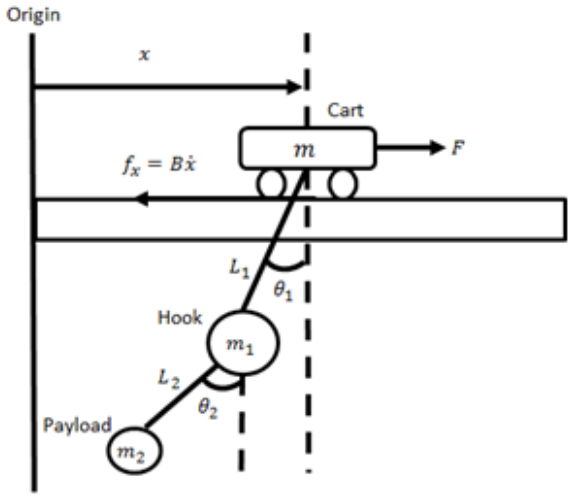

Figure 2. Schematic diagram of a double-pendulum overhead crane system

The dynamic model of the double-pendulum overhead system is obtained through the Euler-Lagrange method. The Euler-Lagrange method involves the total kinetic and potential energies of the system. Euler-Lagrange equation is given as:

$$L_a = K - P \tag{1}$$

$$\frac{d}{dt}\left(\frac{\partial L_a}{\partial \dot{q}}\right) - \frac{\partial L_a}{\partial \dot{q}} = T_i \tag{2}$$

where L_a is the Lagrangian operator, K and P are the total kinetic and potential energies, q_i is the generalised coordinate of the system and T_i is the resultant force acting on the cart.

Using Equations (1) and (2), the mathematical equation is derived as:

$$(m + m_1 + m_2)\ddot{x} + (m_1 + m_2)(L_1\ddot{\theta_1}\cos\theta_1) - (m_1 + m_2)\left(L_1\dot{\theta_1}^2 sin\theta_1\right) + m_2L_2\dot{\theta_2}^2\sin\theta_2 - (m + m_1 + m_2)\dot{x} + (m_1 + m_2)\left(L_1\dot{\theta_1}\cos\theta_1\right) + m_2L_2\dot{\theta_2}\cos\theta_2 = F - f_x \tag{3}$$

$$(m_1 + m_2)\left(L_1\ddot{x}\cos\theta_1 + L_1{}^2\ddot{\theta_1}\right) + m_2L_1L_2\ddot{\theta_2}\cos(\theta_1 - \theta_3) + m_2L_1L_2\dot{\theta_2}^2\sin(\theta_1 - \theta_2) + (m_1 + m_2)(gL_1\sin\theta_1) = 0 \tag{4}$$

$$m_2L_2{}^2\ddot{\theta_2} + m_2L_1L_2\ddot{\theta_1}\cos(\theta_1 - \theta_2) - m_2L_1L_2\dot{\theta_1}^2\sin(\theta_1 - \theta_2) + m_2L_2\ddot{x}cos\theta_2 + m_2gL_2\sin\theta_2 = 0 \tag{5}$$

2.2 Simulation and Experimental Setup

2.2.1 Simulation

A Simulink block diagram was developed based on Equations (3), (4) and (5). Figure 3 shows the Simulink block diagram of the double-pendulum overhead crane system.

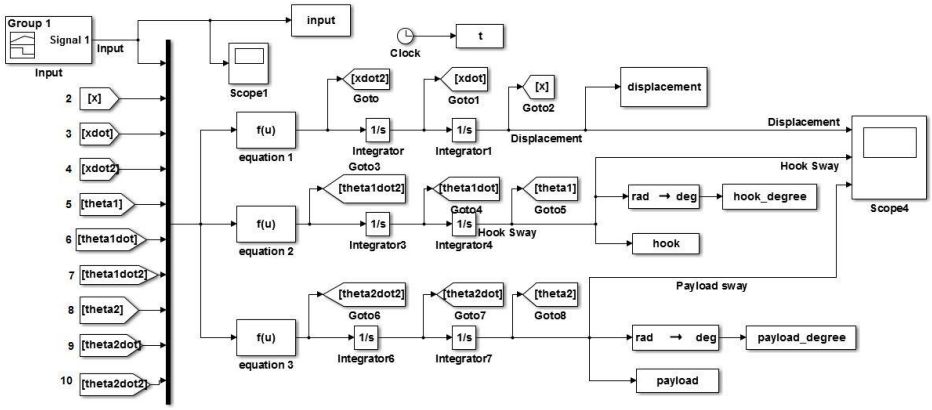

Figure 3. Simulink block diagram for the double-pendulum overhead crane system

2.2.2 Experiments

Figure 4 shows the experimental setup of a double-pendulum overhead crane system. The laboratory crane system is an overhead crane system manufactured by INTECO. It is a 3-Dimensioanl (3D) crane with a dimension of length, width and height of 1.0 m respectively. Figure 5 shows the input signal for both simulation and experiment and Table 1 shows the system parameters that are used in this work that corresponds to the laboratory crane.

Figure 4. Experimental setup of a double-pendulum overhead crane system

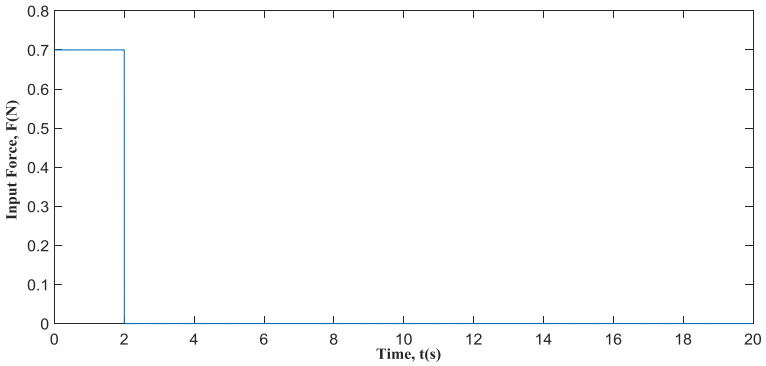

Figure 5. Input signal for simulation and experiment

Table 1. System parameters

Symbols	Descriptions	Values
m	Cart mass	1.155 kg
m_1	Hook mass	0.200 kg
m_2	Payload mass	0.100 kg
L_1	Hook length	0.400 m
L_2	Payload length	0.200 m
B	Coefficient of friction between cart and surface	100 kgs^{-1}/m
g	Gravitational force	9.81 ms^{-2}

3. INPUT SHAPING

Input shaping [1, 9, 14, 16-18] is a method used to reduce system vibration/oscillation. An input shaper consists of a series of impulse signal with amplitude, A_i at specified time location, t_i . Input shaping does not required feedback from the system and it is established based the estimated natural frequencies, ω_n and the damping ratio, ζ of the system [5, 16-18, 22]. Input shaping helps to filter out unwanted signal such as the vibration and the command generated by operators [1, 5, 17-18]. This will reduce the payload sway of the system and also reduce the completion time of a task [1]. There are also several researches using Zero Vibration (ZV), Zero Vibration Derivative (ZVD), Zero Vibration Derivative-Derivative (ZVDD) and Specified Insensitivity (SI) [5] shapers as control methods to solve the payload sway and double-pendulum dynamics. ZV is two-impulse signal, ZVD is a three-impulse signal whereas ZVDD is a four-impulse signal. Figure 6 indicates the process of input shaping.

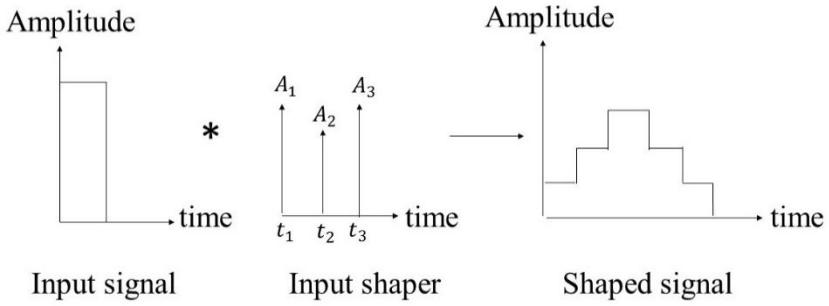

Figure 6. Process of input shaping

ZV, ZVD and ZVDD input shapers are proposed in this paper. The natural frequency, ω_n can be obtained using the Fast Fourier Transform (FFT) while the damping ratio, ζ can be obtained by using the Curve Fitting Toolbox (CFTOOL) in MALTAB. The amplitude, A_i and the time location, t_i of the ZV, ZVD and ZVDD impulse signals can be calculated based on the formula in Table 2.

Table 2. Formula for ZV, ZVD and ZVDD shapers

Type of shaper	Formula
ZV	$\begin{bmatrix} A_i \\ t_i \end{bmatrix} = \begin{bmatrix} A_0 & A_1 \\ t_0 & t_1 \end{bmatrix}$
ZVD	$\begin{bmatrix} A_i \\ t_i \end{bmatrix} = \begin{bmatrix} A_0 & A_1 & A_2 \\ t_0 & t_1 & t_2 \end{bmatrix}$
ZVDD	$\begin{bmatrix} A_i \\ t_i \end{bmatrix} = \begin{bmatrix} A_0 & A_1 & A_2 & A_3 \\ t_0 & t_1 & t_2 & t_3 \end{bmatrix}$

where

$$A_0 = \frac{1}{1+3K+3K^2+K^3}, \quad A_1 = \frac{3K}{1+3K+3K^2+K^3}$$
$$A_2 = \frac{3K^2}{1+3K+3K^2+K^3}, \quad A_3 = \frac{K^3}{1+3K+3K^2+K^3}$$
$$t_0 = 0, \quad t_1 = \frac{\pi}{\omega_d}, t_2 = \frac{2\pi}{\omega_d}, t_3 = \frac{3\pi}{\omega_d}$$
$$K = e^{-\frac{\zeta\pi}{\sqrt{1-\zeta^2}}} \quad \text{and} \quad \omega_d = \omega_n\sqrt{1-\zeta^2}$$

4. RESUTS AND DISCUSSIONS

This section provides a detail analysis on the results obtained from both the simulation and experiment. Initially, the verification of the dynamic model was carried out by comparing the simulation and experimental results. Next, design and analysis of the ZV, ZVD and ZVDD shapers for sway reduction of a double-pendulum crane is discussed.

4.1 Model Verification

Figures 7 and 8 show the cart displacement and hook sway respectively for both simulation and experiment. In the simulation, it was noted that the cart displacement showed some oscillations after the applied force was removed. However, the oscillation did not occur in the experiment. It was shown that the differences in the simulation and experiment of the cart displacement are small within 0.34% - 0.93%. The transient response specifications in terms of the rise time and settling time of the cart displacement were almost similar for both simulation and experiment. The results on the cart displacement and hook sway were tabulated in Table 3. It can be shown that the simulation results with the dynamic model is in agreement with the laboratory crane. Thus, that the derived model is acceptable can be used for control design with confidence.

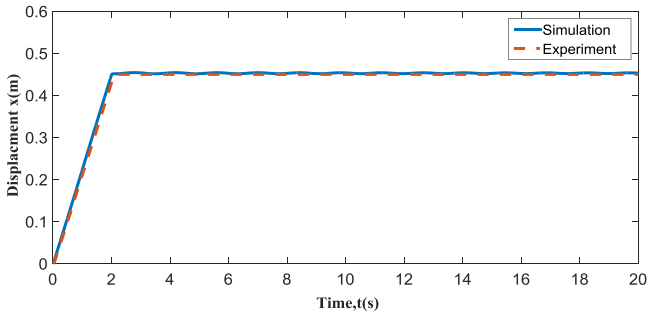

Figure 7. Cart displacement for both simulation and experiment

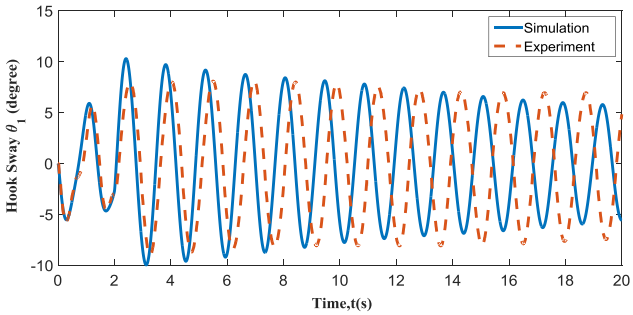

Figure 8. Hook sway for both simulation and experiment

Table 3. Simulation and experimental Formula for ZV, ZVD and ZVDD shapers

	Cart displacement			Maximum hook sway (deg)	Maximum payload sway (deg)
	Displacement (m)	Rise time (sec)	Settling time (sec)		
Simulation	0.4538	1.6031	1.9804	10.2953	13.8110
Experiment	0.4496	1.6443	2.0590	8.9650	-

4.2 Input Shaping

After the model verification, the FFT and the Curve Fitting Toolbox (CFTOOL) were used to obtain the natural frequency, ω_n and the damping ratio, ζ of the system based on the hook sway. Figures 9 and 10 show the FFT and the CFTOOL for the hook sway. Based on the analyses, the natural frequency of the system, $\omega_n \approx 2\pi(0.6997) \approx 4.396$ rad/s and the damping ratio, $\zeta = 0.01391$ were obtained. The ZV, ZVD and ZVDD input shaper was later designed based on the natural frequency and the damping ratio. Table 4 shows the amplitude, A_i and time location of the signal, t_i of the ZV, ZVD and ZVDD shapers.

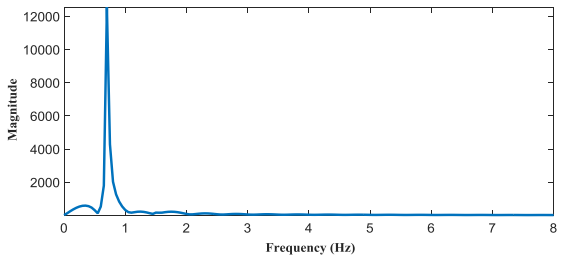

Figure 9. FFT of hook sway

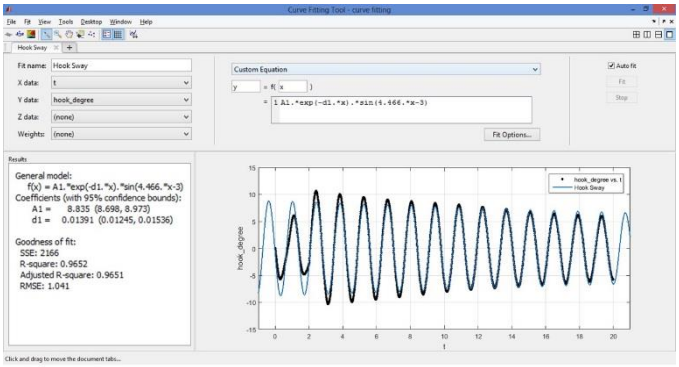

Figure 10. CFTOOL for hook sway

Table 4. Magnitudes and time locations of ZV, ZVD and ZVDD shapers

Type of input shaper	Amplitude and time location
ZV	$\begin{bmatrix} A_i \\ t_i \end{bmatrix} = \begin{bmatrix} 0.5109 & 0.4891 \\ 0 & 0.7035 \end{bmatrix}$
ZVD	$\begin{bmatrix} A_i \\ t_i \end{bmatrix} = \begin{bmatrix} 0.2610 & 0.4998 & 0.2392 \\ 0 & 0.7035 & 1.4070 \end{bmatrix}$
ZVDD	$\begin{bmatrix} A_i \\ t_i \end{bmatrix} = \begin{bmatrix} 0.1334 & 0.3830 & 0.3666 & 0.1170 \\ 0 & 0.7035 & 1.4070 & 2.1105 \end{bmatrix}$

Figure 11 shows the original and shaped signals with the implementation of the ZV, ZVD and ZVDD shapers. Figure 12 shows the cart displacement after the implementation of the ZV, ZVD and ZVDD input shapers. It was noted that the maximum cart displacement decreased after the implementation of input shaper. This is due to the fact the total energy of the input signal was reduced after the convolution of the input signal and the input shapers.

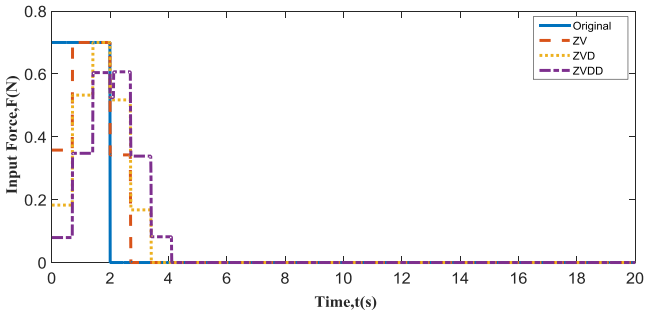

Figure 11. Input signal after the implementation of input shaper

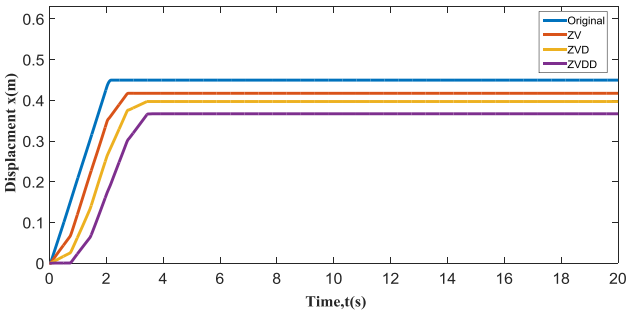

Figure 12. Cart displacement for the experimental double-pendulum overhead crane

Table 5 shows the energy of input signals where it can be seen that the energy decreases after the implementation of the input shaper. The input signal that was convoluted with the ZVDD has the least energy, hence the maximum cart displacement travel was the shortest as compared with other systems. Figure 12 shows that the system responses with the shaped inputs were slightly slower as compared to the original response. The results on the transient response of the system were tabulated in Table 6.

Table 5. Energy of input signal

Source of input signal	Energy, E_s (Joule)
Original	98.0000
ZV	80.5104
ZVD	71.8976
ZVDD	63.7099

Table 6. Transient response specifications of the system

System	Rise time	Settling time	Percent Overshoot
Original	1.6433	2.0590	0
ZV	1.8366	2.6553	3.33
ZVD	1.7949	3.1869	3.67
ZVDD	1.9275	3.3724	0

Figure 13. Transient response specifications of the system

Figure 13 shows the hook sway of the experimental double-pendulum overhead crane system. The maximum hook sway of the system has been reduced significantly after the implementation of the input shapers. Although the ZVDD shaper resulted in a reduced maximum cart displacement, it was very effective in reducing the sway of the system. ZVDD shaper managed to reduce the hook sway up to 69.60%. The results on hook sway were tabulated in Table 7. Figure 14 illustrates the performance of the sway control with ZV, ZVD and ZVDD shapers on sway control.

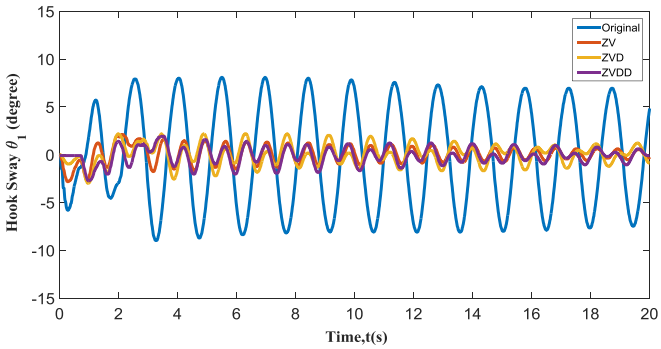

Figure 13. Hook sway for the experimental double-pendulum overhead crane system

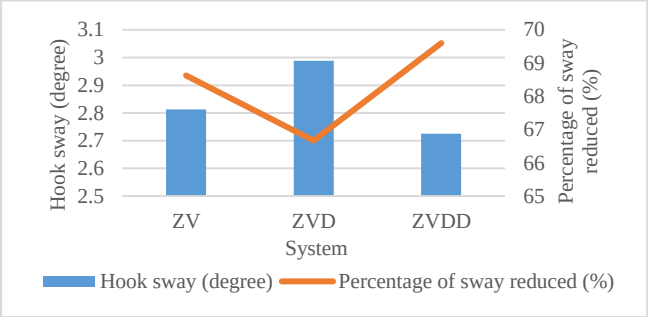

Figure 14. Performance of ZV, ZVD and ZVDD shaper on sway control

Table 7. The hook sway and percentage of hook sway reduced

System	Hook sway (degree)	Percentage of sway reduced (%)
Original	8.9650	-
ZV	2.8125	68.63
ZVD	2.9883	66.67
ZVDD	2.7246	69.60

5. CONCLUSION

A dynamic model of the double-pendulum overhead crane system was derived using the Euler-Lagrange method and verified with a laboratory crane. A good agreement between the dynamic model and the laboratory crane was obtained. The crane dynamics were analysed and the natural frequency and damping ratio were obtained and used in designing several input shapers. Simulation and experimental results showed that the design shapers were able to significantly reduce the hook and payload sway.

REFERENCES

[1] A. Karajgikar, J. Vaughan and W. Singhose, Double-pendulum crane operator performance comparing PD-feedback control and input shaping, *Eccomas Thematic Conference*, Brussels, Belgium, 2011.

[2] D. Qian, S. Tong, B. Yang and S. Lee, Design of simultaneous input-shaping-based SIRMs fuzzy control for double-pendulum-type overhead cranes, *Bulletin of the Polish Academy of Sciences Technical* Sciences, 63(4), 887-896, 2015.

[3] Guo Weiping, Liu Diantong, Yi Jianqiang and Zhao Dongbin, Passivity-based-control for double-pendulum-type overhead cranes, *IEEE Region 10 Conference TENCON 2004*, 546-549, 2004.

[4] M. Kenison and W. Singhose, Input shaper design for double-pendulum planar gantry cranes, *Proceedings of the 1999 IEEE International Conference on Control Applications*, Hawaii, USA, 539-544, 1999.

[5] J. Vaughan, E. Maleki and W. Singhose, Advantages of using command shaping over feedback for crane control, *Proceedings of the 2010 American Control Conference*, Baltimore, USA, 2308-2313, 2010.

[6] M. Zhang, X. Ma, M. Rong, X. Tian and Y. Li, Adaptive tracking control for double-pendulum overhead cranes subject to tracking error limitation, parametric uncertainties and external disturbances, *Mechanical Systems and Signal Processing*, 76–77, 15-32, 2016.

[7] J. Vaughan, D. Kim and W. Singhose, Control of tower cranes with double-pendulum payload dynamics, *IEEE Transactions on Control Systems Technology*, 18(6), 1345-1358, 2010.

[8] D. Qian, S. Tong and S. Lee, Fuzzy-logic-based control of payloads subjected to double-pendulum motion in overhead cranes, *Automation in Construction*, 65, 133-143, 2016.

[9] D. Kim and W. Singhose, Performance studies of human operators driving double-pendulum bridge cranes, *Control Engineering Practice*, 18(6), 567-576, 2010.

[10] M.A. Ahmad, R.M.T. Raja Ismail, M.S. Ramli and N. Hambali, Investigations of NCTF with input shaping for sway control of a double-pendulum-type overhead crane. *International Conference on Advanced Computer Control*, Shenyang, China, 456-461, 2010.

[11] J. Huang, Z. Liang and Q. Zang, Dynamics and swing control of double-pendulum bridge cranes with distributed-mass beams. *Mechanical Systems and Signal Processing*, 54–55, 357-366, 2015.

[12] W. Singhose, D. Kim and M. Kenison, Input shaping control of double-pendulum bridge crane oscillations. *Journal of Dynamic Systems, Measurement, and Control*, 130(3), 034504, 2008.

[13] W. O'Connor and H. Habibi, Gantry crane control of a double-pendulum, distributed-mass load, using mechanical wave concepts, *Mechanical Science*, 4, 251-261, 2013.

[14] D. Kim and W. Singhose, Reduction of Double-Pendulum Bridge Crane Oscillations, *The 8th International Conference on Motion and Vibration Control (MOVIC 2006)*, 27-30 August, Daejeon, Korea, 300-305, 2006.

[15] W.E. Singhose and S.T. Towell, Double-pendulum gantry crane dynamics and control, *Proceedings of the 1998 IEEE International Conference on Control* Applications, Trieste, 1205-1209, 1998.

[16] Kyung-Tae Hong, Chang-Do Huh and Keum-Shik Hong, Command shaping control for limiting the transient sway angle of crane system, *International Journal of Control, Automation and Systems*, 1(1), 43-52, 2003.

[17] M.A. Ahmad, R.M.T.R. Ismail, M.S. Ramli, A.N.K. Nasir and N. Hambali, Feed-forward techniques for sway suppression in a double-pendulum-type overhead crane, *International Conference on Computer Technology and Development*, Kota Kinabalu, Malaysia, 173-178, 2009.

[18] M.A. Ahmad, R.M.T. Raja Ismail, M.S. Ramli and N. Hambali, Comparative assessment of feed-forward schemes with nctf for sway and trajectory control of a DPTOC, *International Conference on Intelligent and Advanced Systems*, Kuala Lumpur, Malaysia, 1-6, 2010.

[19] L. Ramli, Z. Mohamed, A.M. Abdullahi, H.I. Jaafar and I.M. Lazim, Control strategies for crane systems: a comprehensive review, *Mechanical Systems and Signal Processing*, 95, 1-23, 2017.

[20] Z.N. Masoud and K.A Alhazza, Command-shaping control system for double-pendulum gantry cranes, *ASME International Design Engineering Technical Conferences and Computers and Information in Engineering Conference*, Washington, USA, 367-375, 2011.

[21] N. Sun, Y. Fang, H. Chen and B. Lu, Energy-based control of double pendulum cranes, *IEEE International Conference on Cyber Technology in Automation, Control, and Intelligent Systems (CYBER)*, Shenyang, China, 258-263, 2015.

[22] X. Xie, J. Huang and Z. Liang, Vibration reduction for flexible systems by command smoothing, *Mechanical Systems and Signal Processing*, 39(1–2), 461-470, 2013.